University Library

MINERVA ACCESS

A gateway to Melbourne's research publications

Minerva Access is the Institutional Repository of The University of Melbourne

Author/s:
Bagherjeri, FA;Ritchie, C;Gable, RW;Bryant, G;Boskovic, C

Title:
Incorporation of Vanadium and Molybdenum into Yttrium-Arsenotungstates Supported by Amino Acid Ligands

Date:
2020-03-01

Citation:
Bagherjeri, F. A., Ritchie, C., Gable, R. W., Bryant, G. & Boskovic, C. (2020). Incorporation of Vanadium and Molybdenum into Yttrium-Arsenotungstates Supported by Amino Acid Ligands. Australian Journal of Chemistry, 73 (3), pp.137-144. https://doi.org/10.1071/CH19326.

Persistent Link:
https://hdl.handle.net/11343/333726

Incorporation of Vanadium and Molybdenum into Yttrium-Arsenotungstates Supported by Amino Acid Ligands

Fateme Akhlaghi Bagherjeri,[A] *Chris Ritchie,*[A,B] *Robert W. Gable,*[A] *Gary Bryant*[C] *and Colette Boskovic*[A D]

[A] School of Chemistry, University of Melbourne, Parkville, 3010, Australia

[B] Current address: School of Chemistry, Monash University, Clayton, 3800, Australia

[C] Centre for Molecular and Nanoscale Physics, School of Applied Sciences, RMIT University, Melbourne, 3001, Australia

[D] Corresponding author. Email: c.boskovic@unimelb.edu.au

Abstract

The preference for incorporation of molybdenum over tungsten into specific sites of a family of yttrium-arsenotungstates with amino acid ligands prompted exploration of the incorporation of other metals, affording three new vanadium-containing (V/W and V/Mo/W) analogues: $K_2(GlyH)_{10}[As_4(V_2W_2)W_{44}Y_4O_{160}(Gly)_8(H_2O)_{12}]\cdot 11Gly$ (**1**), $(MBAH)_9(L\text{-}NleH)_3[As_4(V_2W_2)W_{44}Y_4O_{160}(L\text{-}Nle)_8(H_2O)_{12}]$ (**2**) and $(MBAH)_9(L\text{-}NleH)_3[As_4(V_2W_2)Mo_2W_{42}Y_4O_{160}(L\text{-}Nle)_8(H_2O)_{12}]$ (**3**) (Gly = glycine and L-Nle = L-norleucine, MBAH = 4-methylbenzylammonium). These complexes all possess a tetrametallic oxo-bridged $\{V^{IV}_2W^{VI}_2\}$ central core surrounded by an amino-acid-ligated cyclic oxo-metal framework. X-ray photoelectron, UV-Visible reflectance and electron paramagnetic resonance spectroscopy, together with metal analysis, confirm the incorporation of vanadium into the hybrid polyoxometalates, while single crystal X-ray diffraction analysis supports the location of the vanadium atoms in the central core.

Introduction

Polyoxometalates (POMs) are oxo-bridged coordination clusters of early transition metals in high oxidation states and are dominated by examples containing vanadium, molybdenum and tungsten. They vary widely in nuclearity and structure, but a common feature is the exhibition of multiple, reversible redox processes. The redox versatility of many POMs has afforded applications in oxidation catalysis,[1–3] while the change in colour upon reduction has been exploited in analytical science.[3] In some circumstances, POMs are reduced upon exposure to light due to photoinduced redox processes, which offers potential utility of these materials in photocatalysis and photocolorimetry.[4–6] Heteropolyanions incorporate heteroatoms within the transition-metal-oxo framework, which can be from any of the blocks in the periodic table. Polyoxometalates can also be functionalised by derivitisation with organic ligands.[7,8]

The redox properties of POMs can be tuned by synthesising mixed-metal POMs, for example by replacing some tungsten sites of a polyoxotungstate with molybdenum or vanadium. Ease of reduction generally follows the order V(V) < Mo(VI) < W(VI).[9–11] Examples where some of the molybdenum or tungsten centres have been substituted for vanadium(IV or V) include the paradigmatic Keggin (e.g. $[PV_xM_{12-x}O_{40}]^{n-}$ (M = Mo, W)) and Wells-Dawson (e.g. $[P_2V_xM_{18-x}O_{62}]^{n-}$) POMs, allowing tuning of the redox properties.[12–18] Cronin *et al.* reported the mixed-valence vanadium-substituted species, $[Mo_{11}V^{V}_{5}V^{IV}_{2}O_{52}(\mu_9\text{-}SO_3)]^{7-}$, which has seven vanadium atoms in two oxidation states.[19] The $[ZMo_{3-x}V_xW_9O_{40}]^{n-}$ (Z = P and Si) and $[P_2VMoW_{16}O_{62}]^{8-}$ polyanions are rare examples of POMs with three different "addenda" metals, with Mo and V centres occupying specific sites in the parent Keggin and Wells-Dawson polyoxotungstate structures.[11,20] Vanadium-substituted mixed-metal POMs can be excellent catalysts for oxidation reactions in organic syntheses.[16–18]

Previously, we have introduced a fascinating and structurally versatile family of yttrium-polyoxotungstates (Fig. 1) with glycine (Gly) or L-norleucine (L-Nle) ligands (Chart

1): $[As_4\{M_4\}W_{44}Y_4O_{160}(AA)_8(H_2O)_{12}]^{n-}$ (M = Mo or W, AA = gly or Nle). For the norleucine-containing compounds, 4-methylbenzylammonium (BMAH) and related arylammonium countercations have proved particularly useful, affording samples of large single crystals.[21–23] While the amino acid/yttrium-polyoxotungstate peripheral framework is preserved in all members of the family, there is some variation in the identity of the metal centres that comprise the central oxo-bridged core, with molybdenum centres occupying these sites in some previously reported complexes (Fig. S1). The tetrametallic central core is the preferred site for reduction and some analogues are very easily reduced, affording 2e-reduced analogues with the additional two electrons occupying a molecular orbital that is delocalised over a unit that is formally $\{Mo^{V}_2M^{VI}_2O_4\}$ (M = Mo or W).[21,22] These reduced compounds exhibit a characteristic "heteropoly blue" colour compared to the white of the parent oxidised species.[24,25] The present work describes the incorporation of vanadium into this hybrid-POM family and the influence of this substitution on the properties of the new compounds. The competitive incorporation of both vanadium and molybdenum was also explored to elucidate the relative preference for substitution of these metals into this versatile polyoxotungstate framework.

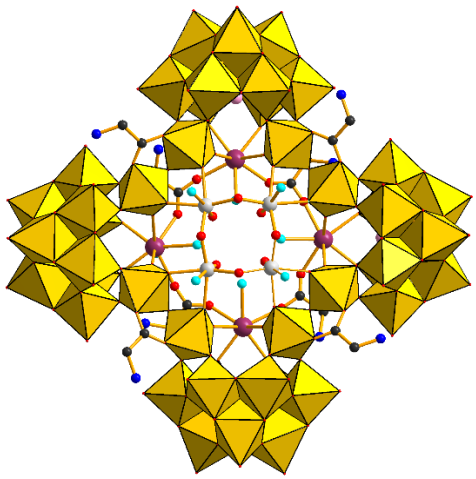
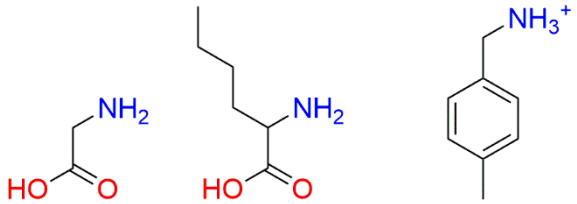


Fig. 1. Structural representation of idealised hybrid polyoxometalate $[As_4(M^{VI}_4)W^{VI}_{44}Y_4O_{160}(Gly)_8(H_2O)_{12}]^{8-}$ (M = Mo, W). Color code: WO_6 octahedra, yellow; Y, violet; disordered Mo/W, grey; As, pale blue; C, black; N, dark blue; O, red; aqua ligands, cyan.



Gly Nle MBAH

Chart 1

Experimental

Materials

All manipulations were performed under aerobic conditions, using materials as received.

Synthesis

*$K_2(GlyH)_{10}[As_4(V_2W_2)W_{44}Y_4O_{160}(Gly)_8(H_2O)_{12}]\cdot 11Gly$ (**1**)*

Solid $K_{14}[As_2W_{19}O_{67}(H_2O)]$ (0.5263 g, 0.1000 mmol) was dissolved in 1 M glycine solution (20 ml, 4.0 mmol) at pH 2.2, with this pH maintained during the dissolution by addition of concentrated HCl (37 %). To this solution was added $VOSO_4$ (0.0270 g, 0.163 mmol) while maintaining the pH at 2.2 using 3 M HCl. Solid $Y(NO_3)_3\cdot 6H_2O$ (0.0626 g, 0.163 mmol) was then added and the pH of the resulting solution was again adjusted to 2.2. The reaction flask was stored in the dark, affording brown plate-shaped crystals after 1-2 days in 17 % yield (100 mg, 0.007 mmol) based on W. Single crystal X-ray structural analysis suggests the formula **1**$\cdot 72H_2O$ for crystals selected from mother liquor, which partially dehydrate upon air-drying. Anal. calcd (found) for air-dried **1**$\cdot 25H_2O$, $C_{58}H_{219}N_{29}K_2As_4V_2W_{46}Y_4O_{255}$: C, 4.74 (4.71); H, 1.50 (1.57); N, 2.76 (2.59); K, 0.53 (0.6); V, 0.69 (0.5); As, 2.04 (1.9); Y, 2.42 (2.7). Selected IR (KBr, cm^{-1}): 1728 (w), 1620 (s), 1483 (m), 1408 (m), 1389 (m), 1325 (w), 1248 (w), 1107 (w), 987 (sh), 960 (m), 866 (s), 802 (w), 744(s), 671 (s), 600 (s), 487 (m).

*$(MBAH)_9(L\text{-}NleH)_3[As_4(V_2W_2)W_{44}Y_4O_{160}(L\text{-}Nle)_8(H_2O)_{12}]$ (**2**)*

Solid $K_{14}[As_2W_{19}O_{67}(H_2O)]$ (0.5263 g, 0.1000 mmol) was dissolved in 0.15 M norleucine solution (20 ml, 4.0 mmol) at pH 2.2, with this pH maintained during the dissolution by addition of concentrated HCl (37 %). To this solution was added $VOSO_4$ (0.0270 g, 0.163 mmol) while maintaining the pH at 2.2 using 3 M HCl. Solid $Y(NO_3)_3\cdot 6H_2O$ (0.0626 g, 0.163 mmol) was then added and the pH of the resulting solution was again adjusted to 2.2. After allowing the reaction mixture to stand for one hour, 4-methylbenzylamine (50 µl, 0.39 mmol) was added while maintaining the pH at 2.2 using 3 M HCl. The reaction solution was stirred for 10 minutes and then stored in the dark. A few brown tetrahedral-shaped crystals formed over the course of 7-10 days. Single crystal X-ray structural analysis suggests the formula **2**$\cdot 87H_2O$ for

crystals selected from mother liquor, which partially dehydrate upon air-drying. A collection of crystals was handpicked for elemental analysis, but it was not possible to obtain a pure bulk sample for spectroscopy. Anal. calcd (found) for air-dried **2**·20H_2O, $C_{138}H_{304}N_{20}As_4V_2W_{46}Y_4O_{214}$: C, 11.14 (11.6); H, 2.06 (1.7); N, 1.88 (1.9); V, 0.68 (0.4); As, 2.01 (2.1); Y, 2.39 (2.2).

*$(MBAH)_9(L\text{-}NleH)_3[As_4(V_2W_2)Mo_2W_{42}Y_4O_{160}(L\text{-}Nle)_8(H_2O)_{12}]$ (**3**)*

Solid $K_{14}[As_2W_{19}O_{67}(H_2O)]$ (0.5263 g, 0.1000 mmol) was dissolved in 0.15 M norleucine solution (20 ml, 4.0 mmol) at pH 2.2, with this pH maintained during the dissolution by addition of concentrated HCl (37 %). To this solution were added $Na_2MoO_4·2H_2O$ (0.020 g, 0.082 mmol) and $VOSO_4$ (0.0135 g, 0.082 mmol) while maintaining the pH at 2.2 using 3 M HCl. Solid $Y(NO_3)_3·6H_2O$ (0.0626 g, 0.163 mmol) was then added and the pH of the resulting solution was again adjusted to 2.2. After allowing the reaction mixture to stand for one hour, hydrazinium sulfate solution (0.10 M; 400µl, 0.04 mmol) was added and the solution left overnight. To the resulting blue-purple solution was added 4-methylbenzylamine (50 µl, 0.39 mmol) while maintaining the pH at 2.2 using 3 M HCl and stirred for 10 minutes. Deep blue-purple tetrahedral-shaped crystals formed over the course of 4-5 days in 18 % yield (110 mg, 0.007 mmol) based on W. Single crystal X-ray structural analysis suggests the formula **3**·96H_2O for crystals selected from mother liquor, which partially dehydrate upon air-drying. Anal. calcd (found) for air-dried **3**·20H_2O, $C_{138}H_{304}N_{20}As_4V_2W_{44}Mo_2Y_4O_{214}$: C, 11.27 (11.5); H, 2.08 (1.8); N, 1.90 (1.9); V 0.69 (0.4); Mo, 1.3 (1.1); As, 2.04 (2.1); Y, 2.42 (2.2). Selected IR (KBr, cm^{-1}): 1730 (w), 1624 (s), 1487 (w), 1450 (w), 1425 (w), 1381 (w), 1332 (w), 1118 (w), 982 (sh), 959 (m), 862 (s), 814 (m), 760 (m), 735 (s), 665 (m), 602 (s), 482 (w), 451 (w). ^1H NMR (400 MHz, D_2O): δ 0.87 (m, 33H, CH_3), 1.32 (m, 44H, $(CH_2)_2$), 1.84 (m, 22H, CH_2), 2.33 (s, 24H, CH_3), 3.75 (s, 11H, CH), 4.15 (s, 16H, CH_2), 7.30, 7.35 ppm (br, 32H, ArH).

X-ray Data Crystallography and Structure Determination

Data collection was carried out on a Rigaku Oxford Diffraction SuperNova Dual Wavelength single crystal X-ray diffractometer using Cu-Kα radiation (λ = 1.5418 Å, mirror monochromated) at 130(2) K (Table 1). Using Olex2,[26] the structure was solved with the ShelXT structure solution program using Intrinsic Phasing and refined with the ShelXL refinement package using Least Squares minimization on F^2, using all data.[27,28] All tungsten, yttrium, vanadium and arsenic atoms were refined with anisotropic displacement parameters. It was also possible, for **1**·72H_2O and **2**·87H_2O, to refine all non-solvent carbon, nitrogen and oxygen atoms with anisotropic displacement parameters. For **3**·96H_2O, due to the poor quality of the data, it was only possible to refine the oxygen atoms with isotropic displacement parameters and for the nitrogen and carbon atoms to be given a fixed isotropic displacement parameter of 0.125 $Å^2$. Hydrogen atoms on the zwitterionic glycine ligands were included in calculated positions and refined using the riding model.

For **1**·72H_2O, the four {M_4} central core metal atoms (Fig S1), originally assigned as fully occupied W atoms, showed anomalously large displacement parameters, suggesting partial occupancy of these atoms, or possible disorder. When the occupancy factors were refined, each became significantly smaller than one, and the sum of the four occupancy factors was close to two, while the anisotropic displacement parameters became similar to those of other W atoms. At this point, four strong electron density peaks appeared at positions approximately 0.2 Å above each of the four W centres. Each of these peaks were assigned as partially-occupied V atoms and, on refinement, the sum of the occupancy factors became close to two. This indicates that the core sites are a 1:1 mixture of V and W, in which the two W atoms are distributed over the four sites of the core, while the two V atoms are distributed over four positions situated above the W core plane. Refinement was carried out with the sum of the occupancies for the W atoms, and V atoms, each being restrained to two (Table S1). The

oxygen atoms involved in the V=O and W=O bonds were also included with partial occupancies, with the V=O and W=O distances restrained to 1.59 and 1.63 Å, respectively; the displacement parameters of each component were constrained to be equal. None of the W atoms in the rest of POM showed significant partial occupancy, and accordingly, all were assigned full occupancy during the rest of the refinement. For **2**·87H_2O and **3**·96H_2O the molecules sit around a four-fold axis, with only one core metal centre in the asymmetric unit; the occupancy factors of the W and V atoms refined to values close to 0.5 and so the refinement was continued with the occupancy factors fixed at 0.5. For **2**·87H_2O the oxygen atoms involved in the V=O and W=O bonds were also included with partial occupancies, with the V=O distance restrained to 1.59Å. For **3**·96H_2O the presence of Mo in the bulk sample (2 atoms per molecule) raised the question of the location of the Mo atoms. Although the quality of the data was relatively low, refinement of the metal atoms was sufficiently accurate to suggest likely Mo sites. There did not seem to be any evidence that there was any Mo in the core. However, refining the occupancy factors of all non-core W atoms in the polyanion showed that two W atoms in the {$Y_4M_8L_8$} ring and two W atoms in the {AsM_9} lacunary Keggin triad (Fig. S1) had occupancies less than one, suggesting partial occupancy by Mo. Accordingly, to be consistent with the bulk analysis, these sites were refined as a mixture of W and Mo, with the sum of the occupancy factors for the Mo being fixed at 0.5 for the asymmetric unit. It was possible to find positions for some of the solvent water, but not for any cations or free ligand; all solvent oxygen atoms located were refined with isotropic displacement parameters. The composition of solvent voids was performed using the OLEX2 solvent mask routine[20] on the basis of the chemical analyses of all compounds. The final refinements were carried out using the OLEX2 solvent mask routine to account for the contribution of the unassigned disordered solvent, cations and uncoordinated ligands. The data can be obtained free of charge from the Cambridge Crystallographic Data Centre via

www.ccdc.cam.ac.uk/datarequest/cif. CCDC: 1871286, 1871299 and 1871289 for **1**·72H_2O, **2**·87H_2O and **3**·96H_2O, respectively.

Table 1. Crystallographic Data for Compounds **1**·72H_2O, **2**·87H_2O and **3**·96H_2O

	1·72H_2O	**2**·87H_2O	**3**·96H_2O
Formula	$K_2(C_2H_6NO_2)_{10}C_{16}H_{40}As_4N_8O_{188}V_2W_{46}Y_4(C_2H_5NO_2)_{11}(H_2O)_{72}$	$(C_8H_{12}N)_9(C_6H_{14}NO_2)_3(As_4V_2W_{46}Y_4O_{188}N_8C_{48}H_{136})(H_2O)_{87}$	$(C_8H_{12}N)_9(C_6H_{14}NO_2)_3(As_4V_2Mo_2W_{44}Y_4O_{188}N_8C_{48}H_{136})(H_2O)_{96}$
Formula weight / g mol^{-1}	15553	16094	16090
Crystal system	Monoclinic	Cubic	Cubic
Space group	*P*21/*n*	*F*432	*F*432
a / Å	29.99027(11)	60.0255(3)	59.9386(4)
b / Å	30.96109(17)	-	-
c / Å	29.99685(12)	-	-
α / °	-	-	-
B / °	90.2538(3)	-	-
γ /°	-	-	-
V / $Å^3$	27852.7(2)	216276(4)	215337(4)
Z	4	24	24
T / K	130	130	130
ρ_{calc} / g cm^{-3}	3.709	2.966	2.978
Crystal size	0.118 x 0.074 x 0.055	0.213 x 0.151 x 0.13	0.065 x 0.044 x 0.030
2Θ range for data collection	5.894° to 124.646°	7.214° to 152.336°	6.428° to 153.186°
F(000)	28264.0	177528.0	178368.0
Index ranges	$-34 \le h \le 31$, $-30 \le k \le 35$, $-31 \le l \le 34$	$-73 \le h \le 70$, $-74 \le k \le 63$, $-60 \le l \le 73$	$-73 \le h \le 71$, $-73 \le k \le 32$, $-74 \le l \le 70$
Absorption correction	Multi-scan	Multi-scan	Gaussian
Refinement method	Full-matrix least-squares on F^2	Full-matrix least-squares on F^2	Full-matrix least-squares on F^2
reflns measd	157113	198562	168199
unique reflns	43708	18746	17956
Data/ restraints/ parameters	43708/56/2525	18746/114/686	17956/66/365
R_{int}	0.0418	0.066	0.0953
R_1 [$I > 2\sigma(I)$]	0.0359	0.0379	0.1070
wR_2 (all data)	0.0996	0.1159	0.3880
Goodness-of-fit on F^2	1.003	1.055	1.06
$\Delta\rho_{max,min}$ / e $Å^{-3}$	3.35/-1.79	1.10/-0.46	1.26/-1.72

Other Measurements

Elemental analyses were performed by the Microanalytical Unit, Research School of Chemistry, Australian National University, Australia. Thermogravimetric analyses were performed on a Mettler Toledo thermal analyser. Infrared spectra (KBr disk) were recorded as pressed KBr disks on a Bruker Tensor 27 FTIR spectrometer. ^{1}H NMR spectra were acquired on a Varian MR400 400 MHz spectrometer and referenced to residual HDO. X-ray photoelectron (XPS) spectra were recorded on a Thermo Scientific K-Alpha Photoelectron

Spectrometer system with a monochromated, micro-focused Al K-α X-ray source. Calibration of all spectra was attained by reference to the carbon 1s signal with a binding energy of 285.0 eV. Electronic reflectance spectra were measured on a Thermo Scientific-Evolution 220 UV-Visible spectrometer. Solid state electron paramagnetic resonance (EPR) spectra were recorded on a Bruker CW ELEXYS E 500 spectrometer at 9.86 GHz frequency; a powder sample of 2,2-diphenyl-1-picrylhydrazyl (DPPH, g = 2.0037) was used as an external standard.

Results and discussion

Synthesis

Synthesis of the vanadium-containing hybrid POMs **1**-**3** involved a slight modification of the procedures reported previously for the vanadium-free parent compounds.[21–23] The arsenotungstate precursor $K_{14}[As_2W_{19}O_{67}(H_2O)]$ was dissolved in Gly or L-Nle buffer at pH 2.2. Yttrium nitrate was added to the solution, followed by vanadyl sulfate and the pH adjusted to 2.2 with HCl. After stirring at room temperature for an hour, the clear brown solution was kept in the dark and brown crystals of **1**·$72H_2O$ appeared after 1-2 days in moderate yield. The synthesis of the Nle-containing compounds was similar, however, 4-methylbenzylamine was added, with pH control, to the acidic reaction solution to provide countercations. The resulting mixture was filtered prior to being left to crystallise. A small amount of brown crystals of **2**·$87H_2O$ appeared after 7-10 days, but efforts to synthesize enough bulk sample for full characterization failed. In an effort to explore the competitive incorporation of vanadium versus molybdenum into the hybrid polystungstate framework experiment, precursor $K_{14}[As_2W_{19}O_{67}(H_2O)]$ was dissolved in L-Nle buffer at pH 2.2. Then yttrium nitrate, was added to the solution, followed by sodium molybdate and vanadyl sulfate. Hydrazinium sulfate was added as a reductant, as per the non-vanadium containing analogue.[21,22] The pH was

again maintained at 2.2 during the reaction and the product was obtained by adding 4-methylbenzylamine, followed by filtration. Blue-brown crystals of **3**·96H_2O appeared after 4-5 days and could be isolated in moderate yield.

Compounds **1-3** all incorporate vanadium(IV) ions and all efforts to instead obtain vanadium(V)-containing analogues were unsuccessful. The replacement of vanadyl sulfate with vanadium pentoxide afforded the vanadium(IV) analogues in lesser yield, due to *in situ* reduction. A similar difficulty was encountered previously with molybdenum, with facile *in situ* reduction to molybdenum(V) making it difficult to isolate molybdenum(VI)-containing analogues. Although a molybdenum(VI)-containing analogue could be synthesised from crystallisation in the dark,[22] similar efforts with **1-3** were unsuccessful.

Bulk samples of partially dehydrated **1**·25H_2O and **3**·20H_2O were isolated and studied, but only a handful of crystals of **2**·87H_2O could be obtained and further characterisation was not possible. The formulations of the compounds that are presented were obtained by combining information from single crystal X-ray structural analysis, bulk elemental analysis, thermogravimetry (Fig S2) and integration of the ^{1}H NMR spectra (Fig. S3). The infrared spectra of **1**·25H_2O and **3**·20H_2O (Fig S4) are very similar to those of the previously reported vanadium-free analogues.[21–23]

Structures

Single crystal X-ray diffraction data (Table 1) indicate that compounds **1**·72H_2O, **2**·87H_2O and **3**·96H_2O are isomorphous with previously reported vanadium-free analogues.[21–23] Gly-containing compound **1**·72H_2O, crystallizes in the monoclinic space group $P2_1/n$, while L-Nle-containing **2**·87H_2O and **3**·96H_2O crystallize in the enantiomorphic cubic space group $F432$.

The structure of the hybrid POMs in each compound are based on the $[As_4(M_4)Mo_xW_{44-x}Y_4O_{160}(AA)_y(H_2O)_z]^{n-}$ (M = V/Mo/W) generic unit. This is comprised of four tri-lacunary α-

Keggin $\{AsM_9\}$ moieties linked by a $\{Y_4M_8L_8\}$ ring fragment (L = zwitterionic Gly, **1**; L-Nle , **2** and **3**) surrounding an inner oxo-bridged tetrametallic core (Figs. 2 and S1). Two types of zwitterionic amino acid ligands bridge pairs of tungsten centres or pairs of yttrium centres via carboxylate groups, with the protonated amine groups involved in intramolecular hydrogen bonding to the $\{AsW_9\}$ fragments with N(-H)···O distances of 2.8-3.0 Å. Each of the core metal centres is six-coordinate with *trans*-disposed terminal oxo and aqua ligands.

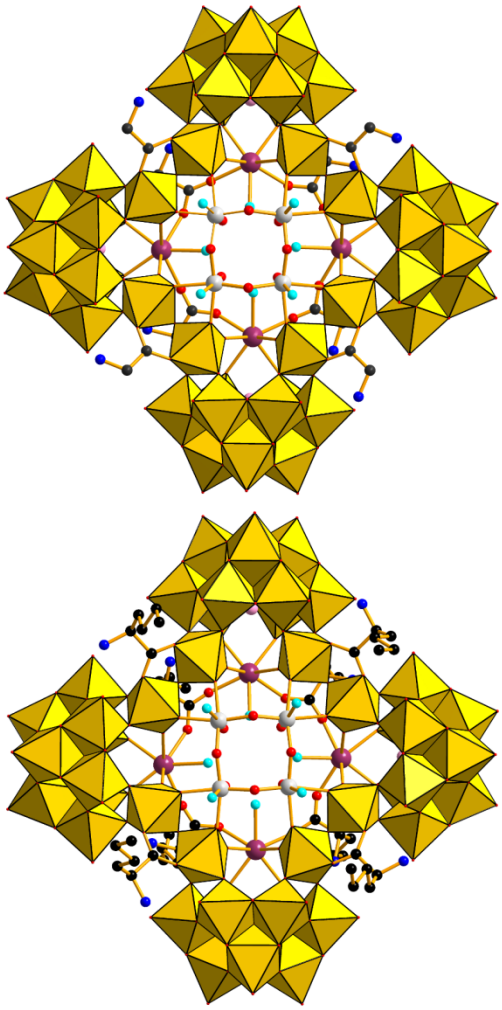


Fig. 2. Structural representations of the molecular structure of the polyanions in **1** (top), **2** and **3** (bottom). Color code: WO_6 octahedra, yellow; Y, violet; disordered V/W or V/Mo/W, grey; As, pale pink; C, black; N, dark blue; O, red; aqua ligands, cyan.

For each of compounds **1**-**3**, the bulk elemental analysis data are consistent with two vanadium centres per complex. The crystallographic data indicate that the vanadium centres are located in a disordered oxo-bridged $\{V_2W_2\}$ central core. Similar positional disorder is common in vanadium-substituted POMs.[19,29–31] The $\{V_2W_2\}$ core exhibits 57(2), 46(2), 52(2), 45(2)% vanadium occupancy for each of the four sites in compound **1** and 50% vanadium occupancy for each position in compounds **2** and **3** (Table S1). The bulk elemental analysis data for the V/Mo/W hybrid **3** indicate two molybdenum centres per POM. The crystallographic data for **3** suggest that there is no molybdenum in the central core, instead there is Mo/W disorder for two positions in the $\{Y_4M_8L_8\}$ ring and two positions in the $\{AsM_9\}$ triad of the tri-lacunary α-Keggin (Fig. S1, Table S1). The refinement of the structure indicates that, similar to the previously reported Mo-containing analogues,[22] there is significant selectivity for the Mo to occupy the POM sites in the order: $\{Y_4M_8L_8\}$ ring > $\{AsM_9\}$ triad > $\{AsM_9\}$ belt.

Bond valence sum (BVS) calculations can give insight into the oxidation states of the metals in the polyoxometalates and BVS calculations for all of the non-core metal sites are consistent with hexavalent tungsten ions. Although the positional disorder in the tetrametallic $\{V_4W_4\}$ core hinders BVS for these sites, the vanadium ions are assumed to maintain tetravalency from the vanadyl starting material and the tungsten centres are assumed to remain hexavalent, consistent with previously reported experimental observations and DFT calculations.[22] In addition, BVS calculations performed for the bridging oxo ligands for all compounds gives values in the range of 1.7-2.2, consistent with an absence of localised protonation to hydroxo ligands.

The crystal packing differs for Gly-containing **1** and Nle-containing **2** and **3**, but is similar to that reported previously for the vanadium-free analogues.[21–23] Compound **1** packs with repeating offset double layers (Fig. S5). Compounds **2** and **3** are isomorphous and the

crystal packing in each case contains cubic cavities surrounded by six hybrid POMs (Fig. S6). For all compounds, the organic cations and molecules of free amino acid, as well as the water molecules, are crystallographically disordered. The total solvent void volume and electron density, calculated using the OLEX2 solvent mask routine, is consistent with the formula obtained from elemental analysis and thermogravimetry.

X-ray Photoelectron Spectroscopy

The W (4f) and V (2p) X-ray photoelectron (XPS) spectra were measured for compounds **1**·25H_2O and **3**·20H_2O and the Mo (3d) spectrum was also measured for compound **3**·20H_2O (Fig. 3). The corresponding binding energies from spectral deconvolution are available in Table S2. The W (4f) spectra for both compounds exhibit only a doublet with binding energies of 35.7-35.9 eV for $4f_{7/2}$ and 37.7-37.9 eV for $4f_{5/2}$. Literature binding energies for the W $4f_{7/2}$ and $4f_{5/2}$ are generally around 35.5 and 37.9 for W(VI), versus 34.1 and 36.7 eV for W(V).[32–34] Thus the XPS data are consistent with hexavalent tungsten in compounds **1** and **3**.

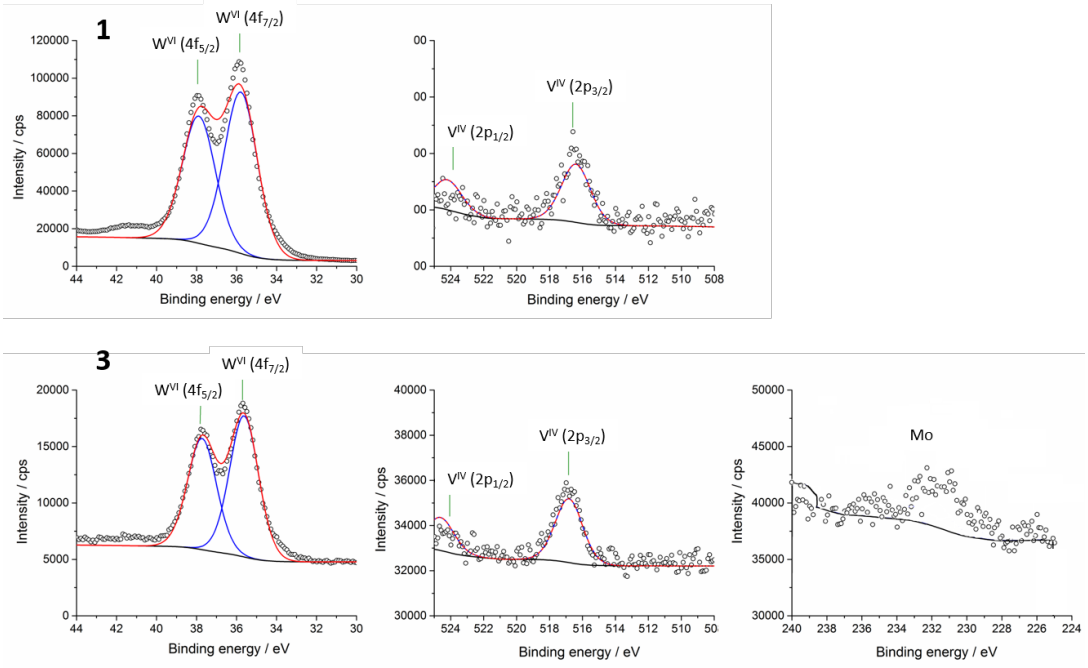


Fig. 3. Tungsten 4f, vanadium 2p and molybdenum 3d XPS and curve fitting results for **1**·25H_2O (top) and **3**·20H_2O (bottom). Experimental data (black circles), peak fitting contributions (blue line), convolution of fitted contributions (red line) and background (black line).

As the amount of vanadium in both compounds is significantly less than tungsten, the corresponding spectra exhibit comparatively poor signal to noise. Generally, only the V ($2p_{3/2}$) peak is clearly observed,[28] due to overlap of the V ($2p_{1/2}$) peak with the O (1s) region (for compounds that contain significant oxygen) and the broadness of the V ($2p_{1/2}$) component compared to the V ($2p_{3/2}$) peak. For compounds **1** and **3** the V ($2p_{3/2}$) peak is evident at 516.4 and 516.3 eV, respectively, consistent with literature binding energies of 515.5-516.8 eV for V(IV), versus values of 517.2-517.9 eV for V(V) and below 515.5 eV for V(III).[32,35]

The Mo (3d) spectrum for **3** is noisy due to the low concentration of molybdenum in the compound, however, peaks are evident, confirming the presence of molybdenum in the sample. It is not possible to deconvolute the measured spectra, although the predominant

features appear to be centred around 232 and 236 eV. Literature binding energies for the Mo $3d_{5/2}$ and $3d_{3/2}$ peaks average around 232.7 and 235.9 eV for Mo(VI); 231.5 and 234.2 eV for Mo(V) and 229.5 and 233.0 eV for Mo(IV).[32,33,35–38] We have previously found that mixed Mo/W analogues of the present compounds underwent X-ray induced photoreduction during XPS measurements, which may also be taking place for compound **3**.[21,22] Thus it is impossible to definitively determine the oxidation state of Mo in **3** from XPS, although the data are consistent with Mo(VI).

Solid state UV-Visible Spectroscopy

To probe the electronic properties of the hybrid POMs, solid-state UV-Visible reflectance spectra were acquired for **1**·25H_2O and **3**·20H_2O diluted in KBr (Fig. 4). The spectra for both compounds exhibit an intense band in the UV region associated with the strong oxo to metal charge transfer bands typical of POMs. The spectra for both compounds feature broad bands in the visible region that are responsible for the brown and purple-blue colour of **1** and **3**, respectively. The band for **1** in the range 360-700 nm can be attributed to intervalence $V^{IV} \rightarrow W^{VI}$ charge transfer and V^{IV} d → d transitions.[11,12,39,40] For **3** the band is very broad between 400 and 800 nm, with a maximum around 660 nm. As well as the transitions mentioned for **1**, there are likely contributions from intervalence $V^{IV} \rightarrow Mo^{VI}$ charge transfer at lower energy than the corresponding $V^{IV} \rightarrow W^{VI}$ bands .[11]

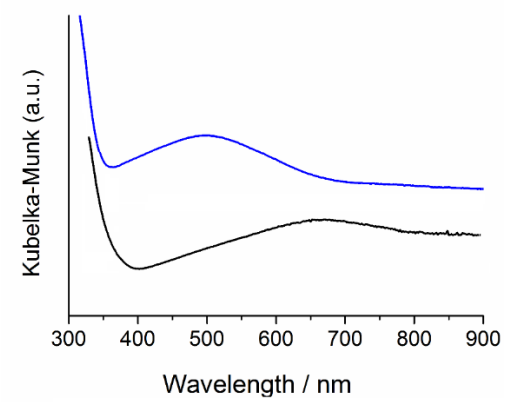


Fig. 4. Solid diffuse reflectance spectra of **1**·25H_2O (blue) and **3**·20H_2O (black) diluted in KBr, plotted as the Kubelka-Munk function.

Electron Paramagnetic Resonance (EPR) Spectroscopy

Powder X-band powder EPR spectra were measured for **1**·25H_2O and **3**·20H_2O at 130 K (Fig. 5). Multiline resonances were observed that are highly characteristic of hyperfine splitting of vanadium(IV) ions (^{51}V; nuclear spin $I = 7/2$, natural abundance 99.76%). The spectra suggest the presence of multiple different localised vanadium(IV) sites in both compounds. The higher resolution spectra obtained at 130 K could be satisfactorily simulated assuming three and two different anisotropic vanadium(IV) sites for compounds **1** and **3**, respectively. The anisotropic g values and hyperfine coupling constants (A) obtained from the simulations are listed in Table S3.

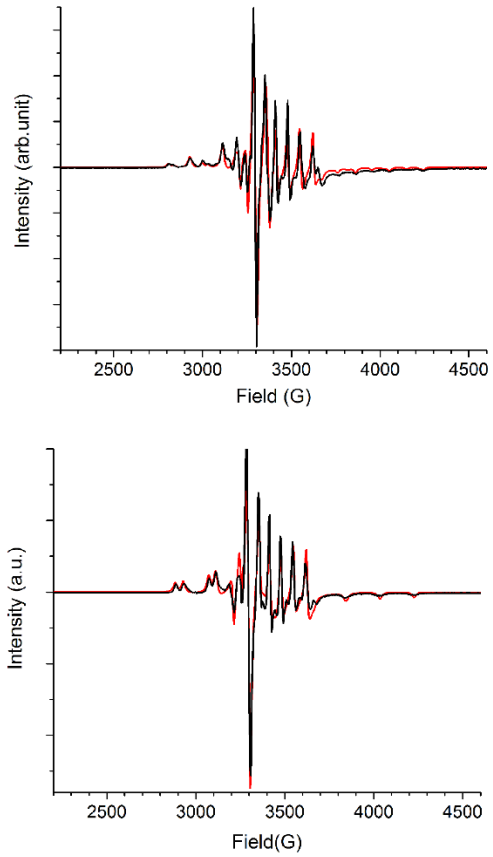


Figure 5. Powder X-band EPR spectrum of **1**·25H_2O (top) and **3**·20H_2O (bottom) at 130 K (black) with simulations (red) as described in the text.

Simulation of the 130 K spectrum for **1** suggests three inequivalent vanadium(IV) ions with relative weights 4:2:1, each with axial ($x = y \neq z$) anisotropy (Table S3: I, II and III) It is not possible to definitively determine the origin of the different types of vanadium(IV) centres in these compounds, but the smallest component might be attributed to the small amounts of a complex with a $\{V_4\}$ core, while the larger components could correspond to complexes with *cis*- and *trans*-disposed $\{V_2W_2\}$ cores. The spectra for **3** can be well simulated assuming only two different vanadium(IV) environments with equal weight (Table S3: I and II), consistent with an equal mixture of complexes with *cis*- and *trans*-disposed $\{V_2W_2\}$ cores. For both compounds, the lower field, parallel (z), region clearly indicates the different centres, while no

differences are apparent in the perpendicular (x, y) region. The centre I in **3** has essentially the same parameters as centre I in **1**, while centre II in **3** is more similar to II and III in compound **1**. For both compounds, g_z is lower than g_x and g_y, which is typical for V^{IV}=O units and has been reported previously for similar vanadyl-containing mixed-metal POMs.[11,14,20,29,30,40,41] It should be noted that the different vanadium environments might also be due to coordination of a ninth disordered amino acid ligand to a core vanadium centre, as has been observed previously for the vanadium-free analogues, however, there is no crystallographic evidence for this in either **1** or **3**.

Concluding remarks

Three new vanadium-containing members of a family of amino-acid-ligated yttrium-polyoxotungstates have been synthesised and characterised. In each case two vanadium(IV) centres are selectively incorporated into the tetrametallic core, generating an oxo-bridged $\{V^{IV}_2W^{VI}_2\}$ unit. This is consistent with previous observations of vanadium-free analogues that found that the central core was both the preferred site for incorporation of molybdenum and the preferred site for reduction, with 2e-reduction affording a $\{Mo^{V}_2W^{VI}_2\}$ core for mixed Mo/W compounds. A competition experiment, with both vanadium and molybdenum in the reaction mixture, revealed the preference for vanadium to occupy the core sites over molybdenum, with some molybdenum instead replacing tungsten in the peripheral POM framework. As a side-note, this experiment generated a rare example of a mixed 3d-4d-5d (V-Mo,Y-W) metal-containing hybrid POM. In the present and previous cases, the presence of d^1 metal ions in the tetrametallic core imparts distinct colours to the hybrid POMs through intervalence charge transfer transitions. The possibilities in terms of the metal substitution and redox chemistry of the apparently modular core unit in this family of hybrid polyanions remains

intriguing. Future explorations of these compounds may focus on the investigation of solution properties, including the redox chemistry and any associated catalytic/photocatalytic activity.

Supplementary Material

Additional structural, spectroscopic and thermogravimetric figures and tabulated data are available on the Journal's website.

Conflicts of Interest

The authors declare no conflicts of interest.

Acknowledgements

We thank the Australian Research Council for funding (DP0877704 and DP110100155) and Prof Lorenzo Sorace for his assistance with simulating the EPR spectra.

References

[1] I. Kozhevnikov, Catalysts for Fine Chemical Synthesis, Volume 2, *Catalysis by Polyoxometalates*, Wiley, **2002**.

[2] I. A. Weinstock, R. E. Schreiber, R. Neumann, *Chem. Rev.* **2018**, *118*, 2680–2717. doi:10.1021/acs.chemrev.7b00444.

[3] Q. Yin, C. L. Hill, *Nat. Chem.* **2018**, *10*, 6–7. doi:10.1038/nchem.2921.

[4] T. Yamase, *Chem. Rev.* **1998**, *98*, 307–326. doi:10.1021/cr9604043.

[5] G. Bernardini, A. G. Wedd, C. Zhao, A. M. Bond, *Proc. Natl. Acad. Sci.* **2012**, *109*, 11552–11557. doi:10.1073/pnas.1203818109.

[6] J. M. Cameron, D. J. Wales, G. N. Newton, *Dalton Trans.* **2018**, *47*, 5120–5136. doi:10.1039/C8DT00400E.

[7] A. Dolbecq, E. Dumas, C.R. Mayer, P. Mialane, *Chem. Rev.* **2010**, *110*, 6009–48. doi:10.1021/cr1000578.

[8] M. -P. Santoni, G. S. Hanan, B. Hasenknopf, *Coord. Chem. Rev.* **2014**, *281*, 64–85. doi:10.1016/j.ccr.2014.09.003.

[9] J. M. Poblet, X. López, C. Bo, *Chem. Soc. Rev.* **2003**, *32*, 297-308. doi:10.1039/b109928k.

[10] L. Parent, P. A. Aparicio, P. De Oliveira, A. L. Teillout, J. M. Poblet, X. López, I. M. Mbomekallé, *Inorg. Chem.* **2014**, *53*, 5941–5949. doi:10.1021/ic500087t.

[11] E. Cadot, M. Fournier, A. Tézé, G. Hervé, *Inorg. Chem.* **2002**, *35*, 282–288. doi:10.1021/ic940908o.

[12] J.J. Altenau, M.T. Pope, R.A. Prados, H. So, *Inorg. Chem.* **1975**, *14*, 417–421. doi:10.1021/ic50144a042.

[13] R. A. Prados, M. T. Pope, *Inorg. Chem.* **1976**, *15*, 2547–2553. doi:10.1021/ic50164a046.

[14] S.P. Harmalker, M.A. Leparulo, M.T. Pope, *J. Am. Chem. Soc.* **1983**, *105*, 4286–4292. doi:10.1021/ja00351a028.

[15] X. López, C. Bo, J. M. Poblet, *J. Am. Chem. Soc.* **2002**, *124*, 12574–82. doi:10.1021/ja020407z.

[16] A.M. Khenkin, L. Weiner, Y. Wang, R. Neumann, *J. Am. Chem. Soc.* **2001**, *123*, 8531–8542. doi:10.1021/ja004163z.

[17] A. M. Khenkin, R. Neumann, *Angew Chem Int Ed Engl.* 2000, 39, 4088–4090. doi:10.1002/1521-3773(20001117)39:22<4088::AID-ANIE4088>3.0.CO;2-%23.

[18] R. Neumann, A. M. Khenkin, *Chem. Commun.* **2006**, 2529–2538. doi:10.1039/b600711m.

[19] H.N. Miras, D.J. Stone, E .J. L. McInnes, R. G. Raptis, P. Baran, G. I. Chilas, M. P.

Sigalas, T. A. Kabanos, L. Cronin, *Chem. Commun.* **2008**, *52*, 4703–4705. doi:10.1039/b811279g.

[20] L. David, C. Crăciun, V. Rusu, O. Cozara, P. Ilea, D. Rusu, *Polyhedron.* **2000**, *19*, 1917–1923.

[21] M. Vonci, F. Akhlaghi Bagherjeri, P. D. Hall, R. W. Gable, A. Zavras, R. A. J. O'Hair, Y. Liu, J. Zhang, M. R. Field, M. B. Taylor, J. Du Plessis, G. Bryant, M. Riley, L. Sorace, P. A. Aparicio, X. López, J. M. Poblet, C. Ritchie, C. Boskovic, *Chem. Eur. J.* **2014***, 20* 14102–14111. doi:10.1002/chem.201403222.

[22] F. Akhlaghi Bagherjeri, M. Vonci, E. A. Nagul, C. Ritchie, R. W. Gable, M. B. Taylor, G. Bryant, S. -X. Guo, J. Zhang, P. A. Aparicio, X. López, J. M. Poblet, C. Boskovic, *Inorg. Chem.* **2016**, *55*, 12329–12347. doi:10.1021/acs.inorgchem.6b02218.

[23] F. Akhlaghi Bagherjeri, C. Ritchie, R.W. Gable, C. Boskovic, *Eur. J. Inorg. Chem.* **2019**, 461–468. doi:10.1002/ejic.201800598.

[24] G. M. Varga Jr., E. Papaconstantinou, M. T. Pope, *Inorg. Chem.* **1970**, *2003*, 662–667. doi:10.1021/ic50085a045.

[25] A. Muller, C. Serain, *Acc. Chem. Res.* **2000**, *33*, 2–10. doi:10.1021/ar9601510.

[26] O. V. Dolomanov, L. J. Bourhis, R. J. Gildea, J. A. K. Howard, H. Puschmann, *J. Appl. Crystallogr.* **2009**, *42*, 339–341. doi:10.1107/S0021889808042726.

[27] G.M. Sheldrick, *Acta Crystallogr.* **2008**, *A64*, 112–122. doi:10.1107/s0108767307043930.

[28] G.M. Sheldrick, *Acta Crystallogr.* **2015**, *C71*, 3–8. doi:10.1107/S2053229614024218.

[29] T. Ueda, M. Ohnishi, M. Shiro, J. Nambu, T. Yonemura, J. F. Boas, A. M. Bond, *Inorg. Chem.* **2014**, *53*, 4891–4898. doi:10.1021/ic402994q.

[30] T. Ueda, J. -I. Nambu, J. Lu, S.- X. Guo, Q. Li, J. F. Boas, L. L. Martin, A. M. Bond, *Dalton Trans.* **2014**, *43*, 5462–73. doi:10.1039/c3dt53161a.

[31] S. Spillane, R. Sharma, A. Zavras, R. Mulder, C.A. Ohlin, L. Goerigk, R. A. J. O'Hair, C. Ritchie, *Angew. Chem. Int. Ed.* **2017**, *56*, 8568–8572. doi:10.1002/anie.201608589.

[32] N. Fuggle, J. C. ; Martensson, *J. Electron Spectros. Relat. Phenomena.* **1980**, *21*, 275–281. doi:10.1016/0368-2048(80)85056-0.

[33] T. H. Fleisch, *J. Chem. Phys.* **1982**, *76*, 780–786. doi:10.1063/1.443047.

[34] W. Feng, Y. Ding, Y. Liu, R. Lu, *Mater. Chem. Phys.* 2006, 98, 347–352. doi:10.1016/j.matchemphys.2005.09.037.

[35] Y. Wang, H. Li, C. Wu, Y. Yang, L. Shi, L. Wu, *Angew. Chem. Int. Ed. Engl.* **2013***, 52*, 4577–81. doi:10.1002/anie.201209497.

[36] L. Wang, P. Yin, J. Zhang, J. Hao, C. Lv, F. Xiao, Y. Wei, *Chem. Eur. J.* **2011**, *17*, 4796–4801. doi:10.1002/chem.201002154.

[37] J. Zhang, W. Li, C. Wu, B. Li, L. Wu, J. Zhang, L. Wu, *Chem. Eur. J.* **2013***, 19*, 8129–8135. doi:10.1002/chem.201300309.

[38] A. K. Iyer, S. C. Peter, *Inorg. Chem.* **2014**, *53*, 653–660. doi:10.1021/ic402858u.

[39] D. P. Smith, M. T. Pope, *Inorg. Chem.* **1973**, *12*, 331–336. doi:10.1021/ic50120a018.

[40] D. P. Smith, H. So, J. Bender, M. T. Pope, *Inorg. Chem.* **1973**, *12*, 685–688. doi:10.1021/ic50121a040.

[41] J. Nambu, T. Ueda, S. -X. Guo, J. F. Boas, A. M. Bond, *Dalton Trans.* **2010**, *39*, 7364–73. doi:10.1039/c003248d.

Graphical Abstract Entry

Vanadium(IV) ions are site-selectively incorporated into a family of yttrium-arsenotungstates with amino acid ligands. The vanadium(IV) ions occupy metal sites in the oxo-bridged tetrametallic core of the polyoxometalate, in preference to molybdenum(V).

